UDC 614.876:666.1 · VIBEENGINEERING · RADIATION DOSIMETRY · GEANT4 MONTE CARLO · 23 JUL 2026 · REV. 5

Calculation of the Personal Skin Dose-Equivalent Rate $\dot{H}_p(0.07)$ from Beta and Gamma Radiation of Uranium Glass Beads

Monte Carlo (Geant4) calculation of the skin dose rate from contact with Czech uranium glass beads ("yellow opal, size 6/0"). Measured specific activities **^{238}U 2.27·10^5 Bq/kg**, **^{235}U 9.9·10^3 Bq/kg**; the uranium is purified — the series secular equilibrium is broken, and the gamma-active daughters of the radium branch are absent. Three packing configurations, spherical bead geometry. The personal skin dose-equivalent rate $\dot{H}_p(0.07)$ on contact ranges from **6.7 ± 0.7** (single bead) to **48 ± 5 µSv/h** (dense mat), almost entirely from beta radiation.

An **interactive calculator with 3D visualisation** accompanies this paper: arbitrary packing geometry, uranium content of the glass and bead size; the model is calibrated against the reference points of this calculation (r.m.s. deviation 0.7 %).

The calculation was performed by an AI agent (Anthropic Claude) under the guidance and control of the operator; the results passed an independent code audit. See §11 "Statement on the use of AI".

⚠ **Disclaimer and need for independent verification.** This material is informational and demonstrational. The reported values are the result of numerical (Monte Carlo) modelling and simplified analytical models, which **may contain methodological errors and inaccuracies in the input data and assumptions**; the resulting estimates are **not metrologically certified measurements**. This material **does not replace** official dosimetry, a certified calculation, or the assessment of authorized radiation-safety specialists, and **must not be used as the sole basis** for decisions affecting health, safety, or regulatory compliance. Before any practical use, the results must be **independently verified by qualified specialists** and, where necessary, by direct measurement with certified instruments. The authors and the operator give no warranty of completeness or accuracy and accept no liability for the consequences of use; the information is used at the reader's own risk.

Sample. Czech uranium glass beads "yellow opal, uranium glass 6/0, 4.1 mm" (art. 31119001/0 8200). Bead mass 63.96 mg (14.710 g / 230 pcs). Measured specific activities: ^{238}U 2.27·10^5 Bq/kg (18.37 g/kg), ^{235}U 9.90·10^3 Bq/kg (0.1237 g/kg); ^{235}U enrichment 0.67 % — essentially natural. The glass shows cerium fluorescence (CeO_2 decolorizer); barium is absent.

Source. The uranium is chemically purified, with minimal radium content: the secular equilibrium of the ^{238}U series is broken at ^{226}Ra, so the gamma-active daughters of the radium branch (^{214}Pb, ^{214}Bi) are absent from the glass. The equivalent skin dose is produced by the short-lived daughters of

the first links of the decay chains, which re-established secular equilibrium with the uranium within months after melting — above all the high-energy beta particle of **^{234m}Pa (E_{max} 2.27 MeV)**.

Method. Geant4 11.2.1[9], electromagnetic physics G4EmStandardPhysics_option4 and the radioactive-decay module G4RadioactiveDecay[11]; the source is distributed over the glass volume (beta self-absorption is included), the spherical bead is in contact with a "skin + adjacent tissue" phantom (layered ICRU soft tissue[8]). The target quantity is the **directional/personal skin dose-equivalent rate $\dot{H}_p(0.07)$** (rate of the personal dose equivalent at 0.07 mm depth ≡ 7 mg/cm², i.e. the epidermal basal layer), averaged over a 1 cm² area per the ICRP/ICRU definition[6]; in the calculation it is taken as the average over the 50–100 μm depth. The normalization was verified with a sanity test (ratio to the analytical inverse-square law = 1.000).

Result. Personal skin dose-equivalent rate $\dot{H}_p(0.07)$ (basal layer, direct contact): **single bead 6.7 ± 0.7 μSv/h**, **chain 18 ± 2 μSv/h**, **dense mat 48 ± 5 μSv/h** (statistical uncertainty < 1 %; the quoted ± uncertainty reflects the ±10 % glass-density uncertainty). The bead shape adds a one-sided upward systematic: the spherical model is a conservative lower estimate, the true value for a single bead up to ~+34 % (full budget in §4). The photon contribution is < 0.2 %; of the emitted beta energy, 55–67 % is absorbed within the glass itself. Under normal handling the dose stays within the limit for the public (skin equivalent-dose limit 50 mSv/year[7]); an appreciable dose accumulates only under many hours of daily direct contact.

1 Sample and objective

Uranium glass is a silicate glass coloured with uranium compounds (typically 0.1–2 wt% U, historically up to tens of percent); it shows a yellow-green colour and bright green fluorescence[1]. The measured uranium mass fraction in the beads studied is **1.85 %** (18.37 g ^{238}U + 0.124 g ^{235}U per kg of glass). The observed cerium fluorescence and the absence of barium indicate that cerium oxide CeO_2 — a common glass decolorizer — was added to the melt: cerium acts not as a colorant but as an oxidizer, converting impurity iron Fe^{2+} (a strong blue-green colorant) into Fe^{3+} (a weak yellow), thereby removing the unwanted tint[2]. Typical CeO_2 additions are 0.025–0.2 wt%[2b]; the calculation adopts ~0.5 % (an upper estimate, negligible for β/γ transport, §3).

Keywords: uranium glass; naturally occurring radioactive material (NORM); purified uranium; secular equilibrium disruption; ^{234m}Pa; skin dose; beta dosimetry; hot-particle effect; Monte Carlo; Geant4; radioactive consumer products.

The aim is to estimate the **equivalent skin dose rate and skin dose from beta and gamma radiation** for direct contact of the beads with skin, in three handling scenarios: (a) one bead, (b) a chain of beads (thread, bracelet), (c) a dense single-row packing — a "mat" (embroidery, dense beadwork). The dose is normalized to the **epidermal basal layer** (depth 50–100 μm, ≈ 5–10 mg/cm²), averaged over a 1 cm² area — the standard definition of the equivalent skin dose[6][7].

2 Radionuclide composition of the source

Per the origin of the glass, its uranium is **chemically purified** (depleted or natural, with minimal radium). Chemical purification of uranium separates its decay products, so the **secular equilibrium of the ^{238}U**

series is broken at ^{226}Ra. Over the lifetime of the object (decades) ^{226}Ra is not appreciably regenerated from ^{230}Th: the half-life of ^{230}Th is 75,584 years[3]. Hence radium and the subsequent chain members are absent — namely **^{214}Pb and ^{214}Bi**, which in radium-bearing material produce the penetrating gamma lines 352 / 609 / 1120 / 1764 keV[4].

Only the short-lived daughters of the **first links** of the ^{238}U and ^{235}U chains are present and radiating, having re-established secular equilibrium with the parent uranium within months of melting:

Table 1. Emitting nuclides of purified uranium. Decay data (half-lives, β endpoints, γ lines) — IAEA Live Chart of Nuclides[3] (ENSDF-based, via API); ICRP-107[4] library in the calculation. The dose rate is computed over two non-overlapping chains (A = 234 and A = 235), not per individual nuclide (see §3).

Nuclide	Spec. activity, Bq/kg	Per bead, Bq	Radiation relevant to skin
Chain A = 234 (from ^{238}U)			
^{234}Th	$2.27 \cdot 10^{5}$	14.52	β, E_{max} ~199 keV + γ 63/93 keV
^{234m}Pa	$2.27 \cdot 10^{5}$	14.52	**β, E_{max} 2.27 MeV** (dominant)
Chain A = 235 (from ^{235}U)			
^{235}U	$9.90 \cdot 10^{3}$	0.633	γ 143/163/185/205 keV + α
^{231}Th	$9.90 \cdot 10^{3}$	0.633	β E_{max} ~389 keV + γ 25–84 keV
No skin dose			
^{238}U, ^{234}U	$2.27 \cdot 10^{5}$	—	α (stopped in glass; tissue range < dead layer)
~~Ra-226 → Bi-214~~	≈ 0	—	~~penetrating series γ~~ — absent (purification)

The dominant contribution to the equivalent skin dose is from beta radiation — chiefly the high-energy beta particle of ^{234m}Pa (E_{max} 2.27 MeV), which penetrates the dead stratum corneum (~70 μm, 7 mg/cm²) and irradiates the living basal layer. This is a direct consequence of the assumed purified uranium (broken secular equilibrium, absence of ^{226}Ra and its gamma-active daughters). Alpha radiation of ^{238}U/^{234}U/^{235}U does not contribute to the skin dose: it is stopped in the glass, and its range in tissue (~40 μm) is less than the dead-layer thickness.

3 Model and calculation method

Monte Carlo and Geant4

The calculation uses the Monte Carlo method — direct statistical modelling of the fate of each individual particle: sampling its birth location, energy, direction and all subsequent interactions with matter down to complete absorption. The particle-transport library **Geant4** (GEometry ANd Tracking, developed at CERN, a standard tool of dosimetry and medical physics) is used, version 11.2.1[9][10]. The *physics list* — the set of interaction models attached to the transport — determines the accuracy:

- **G4EmStandardPhysics_option4** — the most accurate standard configuration of Geant4 electromagnetic physics (recommended for dosimetry). For electrons it includes ionization losses, bremsstrahlung, multiple and single Coulomb scattering; for photons — the photoelectric effect, Compton and Rayleigh scattering, pair production, plus fluorescence and Auger emission. Its range of validity (from ~100 eV) covers the whole energy range of the problem[11].
- **G4RadioactiveDecay** — the radioactive-decay module. For a given nucleus it samples the decay from evaluated nuclear data (a library based on ENSDF / ICRP-107[4][5]): the decay mode, the *full continuous β spectrum* (not a mean energy), the gamma cascade of the daughter, internal-conversion electrons, characteristic X-rays and Auger electrons. The source spectra are not set by hand — they are generated from nuclear data.

Primary source and treatment of the decay chain

The primary particle of each history is the parent ion (e.g. ^{234}Th) at zero kinetic energy, placed at a random point of the glass volume; the decay is sampled immediately. Since β decay conserves the mass number A, the isobaric sub-chain **A = 234** (^{234}Th → ^{234m}Pa → ^{234}U) in secular equilibrium is modelled as a whole: one run with the activity of ^{234}Th reproduces the combined radiation of ^{234}Th and ^{234m}Pa (their activities are equal). Alpha decay changes A, so the chain does not proceed further and the radium series is not regenerated. The **A = 235** chain (^{235}U → ^{231}Th) is modelled analogously. The total dose is the sum of the contributions of the **two non-overlapping chains**, which excludes double counting (see §11 — independent code audit).

Convolution with activities. Each run yields a *response* — the energy absorbed in tissue per decay. The dose rate is obtained by multiplying the response by the measured activity and summing over the chains: $\dot{D} = \Sigma\, A_i \cdot R_i$. Separating "transport ↔ activities" allows the dose to be recomputed when activities are refined without repeating the simulation.

Geometry and phantom

Glass — soda-lime silicate with U 1.84 wt% and Ce ~0.5 % (CeO_2; exact content unknown, negligible effect on β/γ transport at this level), density 2.5 g/cm³[1]. The **bead** 6/0 (rocaille) is modelled as a **sphere Ø4.1 mm with an axial cylindrical hole** (radius 0.93 mm chosen to match the measured mass 63.96 mg); the sphere touches the skin at a single point. The source is distributed over the glass volume, which accounts for **beta self-absorption**: part of the emitted beta particles is absorbed in the glass and never reaches the skin. The calculation gives **55 % of the beta energy absorbed in the glass** for a single bead, rising to **67 %** in a dense packing. The **chain** is 11 spheres in a line at 4.1 mm pitch (touching), the row axis parallel to the skin; scoring is under the central bead. The **mat** is a square lattice of beads at the same pitch.

The "skin + adjacent tissue" phantom. For beta and soft gamma radiation from a contact source, a full-body voxel phantom is not appropriate (beta particles travel ≤ 1 cm into tissue and do not "see" the rest of the body; a voxel model does not resolve the 70 μm layer). Instead a **layered tissue slab** is used: ICRU soft tissue[8], 2 cm thick. The top 0.5 mm is resolved with a fine step (15 μm) and a low secondary-production threshold (5 μm). The absorbed energy is accumulated versus depth and radius within a 1 cm² disk; **electrons** (β particles, internal-conversion and Auger electrons), **decay photons** (γ and characteristic X-rays) and **bremsstrahlung** are scored separately.

Statistics

Statistics: $2 \cdot 10^6$ decays for chain A = 234 and $1 \cdot 10^6$ for A = 235. The statistical uncertainty (1σ) of the basal-layer dose rate is 0.3 % (single bead), 0.6 % (chain), 1.0 % (mat), far below the systematic assumptions (§10). The bremsstrahlung contribution to the skin dose is negligible (< 0.1 %). The credibility of the calculation is justified in §8.

4 Skin dose-equivalent rate $\dot{H}_p(0.07)$: results

Personal skin dose-equivalent rate $\dot{H}_p(0.07)$ (μGy/h = μSv/h, radiation weighting factor $w_R = 1$ for β and γ), direct contact, averaged over 1 cm²:

Table 2. Dose rate versus skin depth, μSv/h. Electron (β) and photon (γ) components separately. Statistical uncertainty ≲ 1 %.

Skin layer	1 bead β	1 bead γ	1 bead Σ	Mat β	Mat γ	Mat Σ
surface 0–5 μm	7.42	0.012	7.43	57.4	0.15	57.6
basal (50–100 μm)	**6.68**	**0.007**	**6.69**	**48.3**	**0.10**	**48.4**
dermis 0.3–0.5 mm	4.82	0.007	4.82	35.2	0.09	35.3
tissue 2–3 mm	0.96	0.003	0.97	7.43	0.05	7.49

Table 3. Skin dose-equivalent rate $\dot{H}_p(0.07)$ (basal layer) by packing configuration. The first uncertainty is statistical (1σ); the "calculation range" accounts for the systematics of bead shape and glass density (§ below).

Configuration	$\dot{H}_p(0.07)$ (sphere), μSv/h	stat. (1σ)	calculation range	electron fraction
single bead	**6.69**	±0.3 %	6.0–9.0	99.9 %
chain (11 beads)	**18.3**	±0.6 %	16–23	99.9 %
dense mat (9×9)	**48.4**	**±1.0 %**	**44–53**	**99.8 %**

Uncertainty budget

The Monte Carlo statistical uncertainty is small (< 1 %); the overall calculation uncertainty is set by the systematic assumptions, chiefly the bead shape. The spherical model gives a **lower estimate** of the skin

dose (compact geometry, point contact, maximal self-absorption); the cylindrical one an upper estimate; the true value for a real rocaille (rounded barrel) lies between them.

Table 4. Uncertainty budget of the calculation (contribution to $\dot{H}_p(0.07)$).

Source	Type	Single bead	Mat
Monte Carlo statistics	random	±0.3 %	±1.0 %
bead shape (sphere ↔ cylinder)	systematic	+34 %	< 1 %
glass density (2.0–3.4 g/cm³)	systematic	±10 %	±10 %
cerium content	systematic	< 1 %	< 1 %
combined (calculation)		**+35 % / −10 %**	**±10 %**

In addition, the result is **linearly proportional to the measured specific activity** of the source: its uncertainty (a measured input) propagates to the dose 1:1 and is not included in the calculation budget — when the activities are refined, the dose is simply rescaled by the corresponding factor.

Field saturation with packing size: the central dose rate grows only while beads are added within the lateral spread of the beta particles (~1 cm). Relative to a single bead: chain ×2.7; mat 5×5 ×7.2, 7×7 ×7.3, 9×9 ×7.2 — **further enlargement of the packing does not increase the dose rate** (saturation is already reached at ~5×5). The skin dose-equivalent rate is **almost entirely due to the electron component** (> 99.8 %); the photon contribution does not exceed 0.2 %, but photons penetrate substantially deeper than beta particles (Fig. 1).

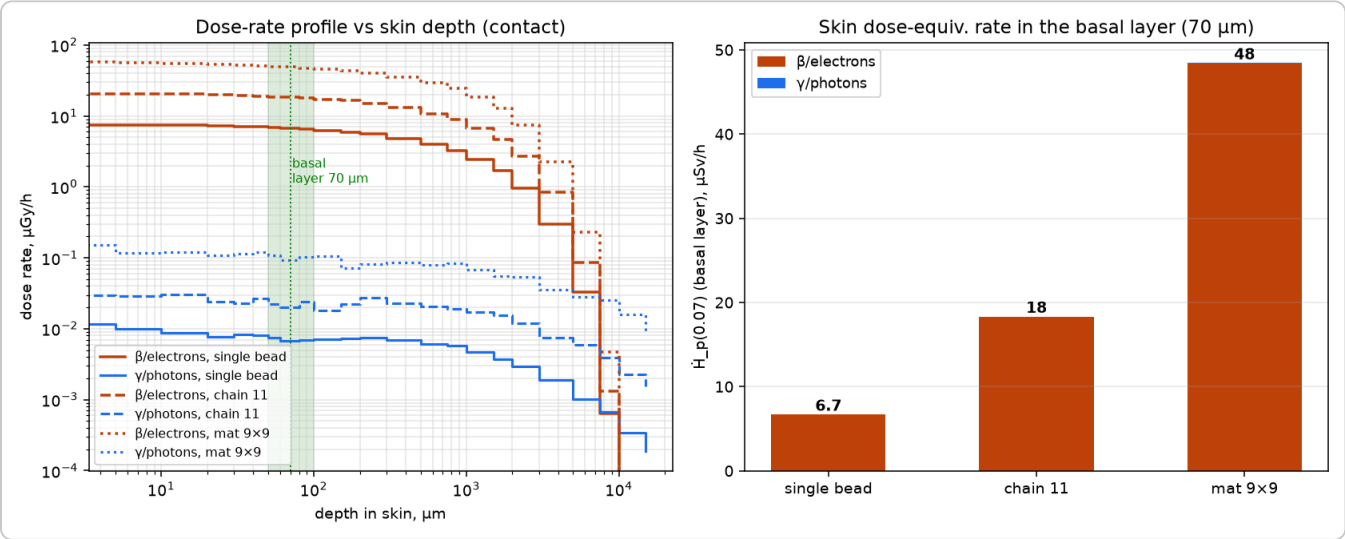

Fig. 1. Left — the absorbed-dose-rate distribution versus depth in the skin phantom for the electron (β particles, conversion and Auger electrons) and photon (γ and X-ray) components; the "single bead", "chain" and "mat" configurations. The green band marks the epidermal basal layer (50–100 µm), for which the skin dose-equivalent rate is normalized. The electron-component dose rate falls off at depths comparable to the extrapolated range of the beta particles (≈ 11 mm for E_{max} = 2.27 MeV ^{234m}Pa); the photon component attenuates much more slowly (exponentially, with the mass attenuation coefficient µ of soft tissue). Right — the basal-layer dose-equivalent rate split into components.

Interactive calculator accompanying this paper. The three configurations above are particular cases. For arbitrary input data an **$\dot{H}_p(0.07)$ calculator with 3D field visualisation** is available.

Inputs: packing geometry (single bead, chain, rectangular N×M array, circular spread) and packing pitch; bead diameter and glass density; uranium mass fraction; averaging area (1, 0.1 or 0.01 cm²); the contact regime, from which the dose per session, the annual dose and the fraction of the skin limits follow.

How it computes. It is not an interpolation of the three published numbers. A point surface dose kernel is constructed and convolved with the emission profile over the emitting face of a bead; the dose rate is summed over all beads and averaged over a disc of the selected area. Bead size and packing pitch therefore enter as parameters of the integration: a bead's contribution grows as the area of its face (beta particles escape only from a layer of ~0.8 mm, see § 7.1), and the uranium content enters linearly.

Accuracy. The kernel is calibrated against seven reference points of the present calculation — a single bead at three averaging areas, the chain of 11, and the 5×5, 7×7 and 9×9 mats; the r.m.s. deviation from Geant4 is **0.68 %**. The comparison table is computed by the calculator page on the fly, with the same code that produces the main result. Outside the calibration range (diameter beyond 2…8 mm and so on) the result is an extrapolation, and the page warns about it explicitly; the disclaimer and the limits of applicability are given there as well.

5 Spatial distribution of the dose-rate field

Three-dimensional distribution of the absorbed dose rate (in a tissue-equivalent medium) around the source for the three configurations. As the packing grows, the localized field of a single bead turns into a quasi-uniform near-surface irradiation layer; the photon component is always broader and orders of magnitude weaker than the electron one.

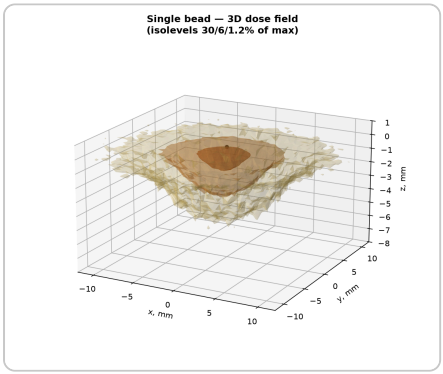

Fig. 2a. Single bead: a localized region of elevated dose extending a few millimetres into the skin.

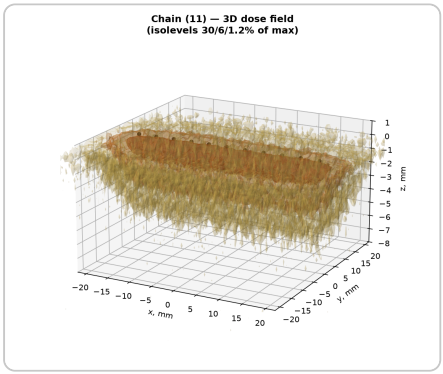

Fig. 2b. Chain: the irradiated region is elongated along the thread.

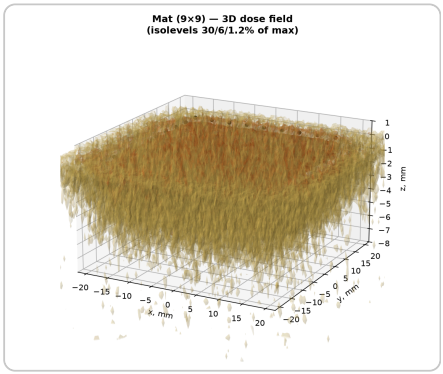

Fig. 2c. Mat: the near-surface tissue layer is irradiated quasi-uniformly.

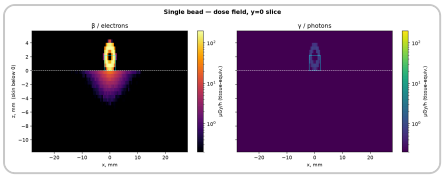

Fig. 3a. Vertical slice of the dose field (electrons left, photons right), single bead. Cyan marks the glass.

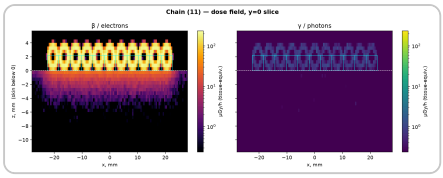

Fig. 3b. Chain.

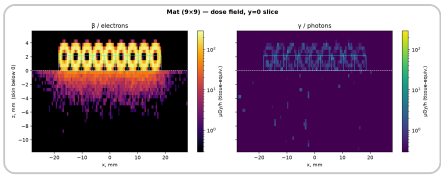

Fig. 3c. Mat. The electron component is confined to the near-surface tissue layer; the photon component spreads over a much larger volume at lower dose density.

6 Local non-uniformity: the "hot particle" effect

The sphere touches the skin essentially at a point, which raises the question of a possible limit exceedance in a microscopic contact spot. However, the skin-dose limit[6][7] is defined precisely as the dose **averaged over a 1 cm² area** — deliberately, because it protects against deterministic skin effects (erythema, necrosis) that require irradiation of a finite tissue volume; the same averaging approach is adopted for discrete radioactive particles (NCRP-130, ICRP). No separate, stricter "local" limit for point contact is introduced.

Quantitatively: the basal-layer dose averaged over a disk of ever smaller area under the contact point rises from the regulatory value of 6.7 μSv/h (1 cm²) to 27 μSv/h over 0.01 cm² (Fig. 4). The peak-to-average (1 cm²) ratio is **×4.1**. Even this peak local value (tens of μSv/h) is orders of magnitude below the levels at which deterministic skin effects occur: the erythema threshold (~3 Gy) at 27 μGy/h would be reached only after ~10^5 hours of continuous contact. Thus the local non-uniformity of the field does not lead to a limit exceedance.

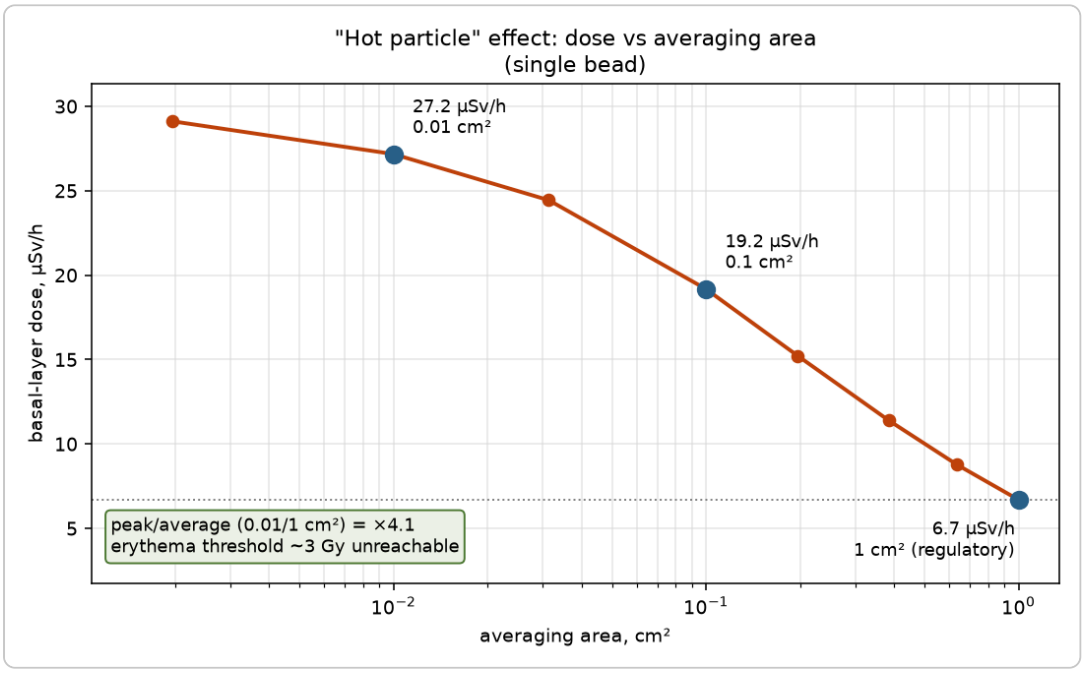

Fig. 4. Single bead: basal-layer dose averaged over a disk, as a function of the averaging area. The 0.01, 0.1 and 1 cm² (regulatory) areas are marked. The peak under the contact point exceeds the regulatory 1 cm² average by ~4×, while remaining orders of magnitude below the threshold of deterministic effects.

7 Verification by a classical method

To check both the order of magnitude and the absolute value independently of Geant4, a classical (semi-analytical) estimate was made, "from simple to accurate": first a closed-form formula for the mat that the reader can reproduce by hand (§7.1), then a volume integral over the sphere with two variants of the dose kernel (§7.2).

7.1. Equivalent dose rate $\dot{H}_p(0.07)$ of the dense packing: closed-form (semi-infinite plane source)

The dense mat is laterally much larger than the beta range (the extrapolated range of the ^{234m}Pa β, E_{max} = 2.27 MeV, in tissue ≈ 1.1 g/cm² ≈ 11 mm; the 9×9 mat ≈ 37 mm), so it is legitimate to approximate it as an **infinite uniform β-active plane of glass**. The dose rate at the surface of a semi-infinite uniform source equals *half* the equilibrium rate in an infinite medium[17] (energy splits equally "up/down"), attenuated to the basal-layer depth:

$$\dot{D}_p(0.07) = \tfrac{1}{2} \cdot \Sigma_i C_{v,i} \cdot \bar{E}_i \cdot e^{-\nu_i \sigma} \cdot k$$

- $C_{v,i}$ — specific activity of nuclide i, Bq/kg (Table 1);
- $\bar{E}_i$ — mean energy of the β spectrum, MeV (IAEA/ICRP-107);
- $\nu_i = 16 \cdot (E_{max,i} - 0.036)^{-1.4}$ — the beta attenuation coefficient, cm²/g (Loevinger empirical[16][17]);
- $\sigma = \rho_{tissue} \cdot d = 1.03\ g/cm^3 \times 7.0 \cdot 10^{-3}\ cm = \mathbf{7.21 \cdot 10^{-3}\ g/cm^2}$ — the mass depth of the basal layer (70 μm);
- k — conversion (Bq/kg)·MeV → μGy/h: $k = 1.602 \cdot 10^{-13}$ J/MeV × $3.6 \cdot 10^9$, i.e. $\dot{D}_\infty[\mu Gy/h] = C_v \cdot \bar{E} \cdot \mathbf{5.767 \cdot 10^{-4}}$.

Worked example for the dominant ^{234m}Pa (four lines on a calculator):

1. $\nu = 16 \cdot (2.27 - 0.036)^{-1.4} = 16 \cdot (2.234)^{-1.4} = 16 / 3.08 = \mathbf{5.19\ cm^2/g}$;
2. $\nu\sigma = 5.19 \times 7.21 \cdot 10^{-3} = 0.0374$; $e^{-0.0374} = 0.963$;
3. $\dot{D}_\infty = 2.27 \cdot 10^5 \times 0.819 \times 5.767 \cdot 10^{-4} = \mathbf{107.2\ \mu Gy/h}$;
4. contribution = ½ × 107.2 × 0.963 = **51.7 μGy/h**.

Table 5. Analytical estimate of the mat over all three β nuclides (semi-infinite source model).

Nuclide	C_v, Bq/kg	$\bar{E}$, MeV	E_{max}, MeV	ν, cm²/g	νσ	$e^{-\nu\sigma}$	$\dot{D}_\infty$, μGy/h	$\frac{1}{2} \cdot \dot{D}_\infty \cdot e^{-\nu\sigma}$
^{234m}Pa	$2.27 \cdot 10^5$	0.819	2.27	5.19	0.037	0.963	107.2	51.7
^{234}Th	$2.27 \cdot 10^5$	0.060	0.199	202.8	1.462	0.232	7.86	0.91
^{231}Th	$9.90 \cdot 10^3$	0.163	0.389	68.7	0.496	0.609	0.93	0.28
Sum (hand estimate of the mat)								**52.8**

Uncertainty. The result is dominated by ^{234m}Pa (the factor $e^{-\nu\sigma} \approx 0.96$ barely matters). The governing contributions are the specific activity (HPGe, u ≈ 10 %) and the mean β energy (u ≈ 10 %): $u_{rel} = \sqrt{(0.10^2 + 0.10^2)} \approx 14$ %. Result: $\dot{D}_p(0.07) \approx 53 \pm 7$ **µGy/h**.

Analytical estimate 53 ± 7 µGy/h vs Monte Carlo 48.4 µGy/h — agreement +9 % (within uncertainty). A closed-form formula done on paper reproduces the MC result for the mat. The slight overestimate is expected: a real bead layer has finite thickness (~0.4 g/cm², comparable to the range), whereas the "semi-infinite" model assumes an infinitely thick source and slightly over-counts the contribution of deeper layers.

7.2. Equivalent dose rate $\dot{H}_p(0.07)$ of the single bead: dose-kernel integral over the sphere

A single bead is small compared with the beta range, so the semi-infinite approximation does not apply to it. For it (and the intermediate packings) a beta **point-dose kernel** was used, integrated over the glass volume of the sphere with self-absorption; the chain and mat are obtained by superposition of spheres on a lattice:

$$\dot{D}(r) = a\cdot\bar{E}\cdot\nu \,/\, (4\pi\, I)\cdot \Phi(\nu\cdot m) \,/\, r^2,\quad I = \int_0^\infty \Phi(u)\,du$$

where m is the mass along the ray (glass + tissue) and r the distance; $a\cdot\bar{E}$ is the total emitted power, $1/(4\pi r^2)$ the geometric spreading of an isotropic point source, $\Phi(\nu\cdot m)$ the dimensionless radial dose fall-off (the dose kernel)[16][18], and the normalization factor $\nu/(4\pi I)$ with $I = \int_0^\infty \Phi(u)du$ is fixed by energy conservation ($\int \dot{D}\cdot\rho\cdot 4\pi r^2 dr = a\cdot\bar{E}$). The dose is evaluated only at target points on the skin (the 1 cm² disk at the basal-layer depth) and summed over all source points in the glass: the $1/(4\pi r^2)$ factor gives the fraction of each point's isotropic emission that reaches the skin **within its solid angle**, and $\Phi(\nu\cdot m)$ attenuates it over the glass path **along the ray to the skin**. Thus not the "whole emission from the sphere" but only the part reaching the skin is counted (electrons going up or sideways have no target on the skin). Two kernels Φ were considered:

- **exponential** $\Phi(x) = e^{-x}$ (I = 1) — the simplest, with an infinite "tail";
- **Loevinger (1956)**[16] $\Phi(x) = c(1-(x/c)\cdot e^{1-x/c}) + x\cdot e^{1-x}$ for $x \le c$; $x\cdot e^{1-x}$ for $x > c$ (c = 2, I = 3.845) — more physical: it falls off more steeply and cuts off near the range.

Table 6. Classical estimate (integral over the sphere) vs Monte Carlo, µSv/h. In parentheses — the ratio to MC.

Configuration	Monte Carlo	exp. kernel	Loevinger kernel
single bead	6.69	6.39 (×0.96)	5.83 (×0.87)
chain (11)	18.3	21.9 (×1.19)	19.9 (×1.09)
mat (9×9)	**48.4**	**74.6 (×1.54)**	**68.5 (×1.41)**

For a single bead the exponential kernel agrees with Monte Carlo to 4 % (6.39 vs 6.69 µSv/h) — the fundamental source is reproduced by a fully independent method. The systematic deviations for packings are analysed in §8.

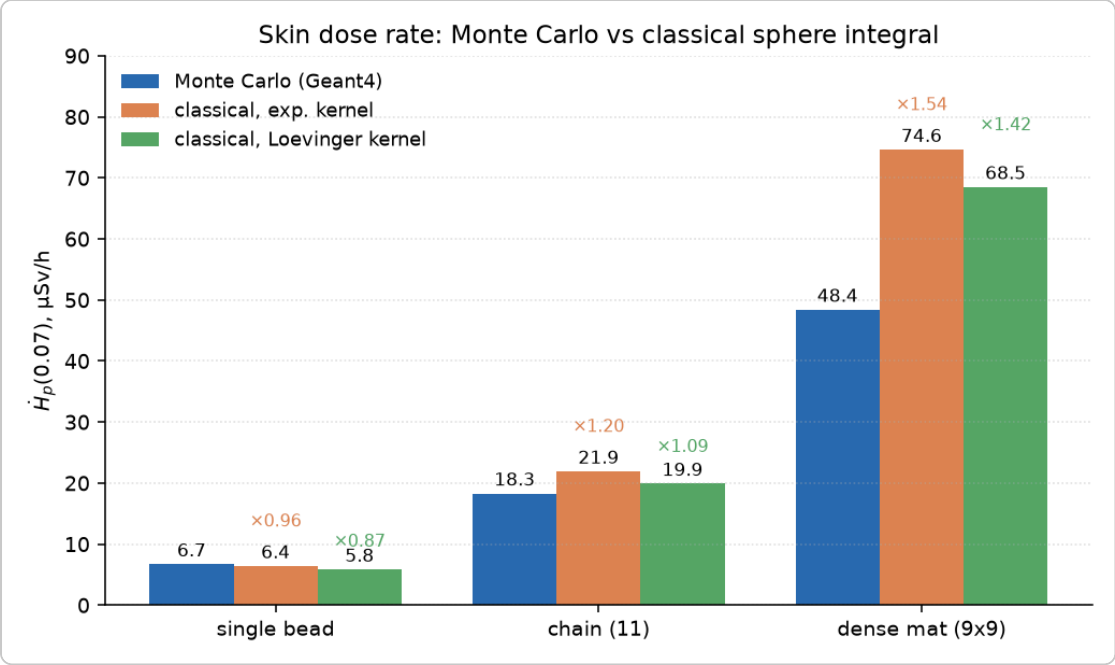

Fig. 5. Classical (semi-analytical) estimate from the sphere vs Monte Carlo. For a single bead the methods agree within 4 %; for extended packings the exponential kernel systematically overestimates the dose, while the Loevinger kernel (cutting off near the range) is markedly closer to MC.

8 Analysis of credibility and discrepancy

The result can be trusted because it is confirmed by several **independent** lines; below is their summary, then the analysis of the single systematic discrepancy.

Table 7. Independent verifications: method, its source, and agreement with Monte Carlo.

What is checked (method and source)	Agreement
Normalization check (sanity test): the computed fluence of a point isotropic γ source in vacuum is compared with the exact inverse-square law $\Phi = N/(4\pi r^2)$ at 10/20/30 cm	computed/analytical ratio = **1.000** — geometry, primary-particle sampling and scoring normalization reproduce the exact solution
First-principles self-consistency of the inputs: measured specific activity ↔ uranium mass fraction (via the specific activity of pure ^{238}U, λN)	$2.27 \cdot 10^5$ Bq/kg → **1.83 wt% U**, matching the independently measured 1.84 %; ^{235}U 0.67 %
Independent closed-form formula for the dense packing (§7.1; semi-infinite source, Loevinger/Cember[16][17])	53 ± 7 µGy/h vs MC 48.4 → **+9 %**
Independent dose-kernel integral over the sphere for a single bead (§7.2; Loevinger kernel[16][18])	6.39 vs MC 6.69 µSv/h → **4 %**

What is checked (method and source)	Agreement
Independent code audit by a separate AI agent (§11): recomputation of doses from raw runs + a Geant4 decay-chain track dump	doses reproduced; a normalization error of the first revision found and fixed

8.1. The "classical ↔ Monte Carlo" discrepancy for packings

The single systematic discrepancy is the growth of the "sphere integral / MC" ratio with packing size: the exponential kernel **×0.96 → ×1.19 → ×1.54**, the Loevinger kernel **×0.87 → ×1.09 → ×1.41**. This is not random scatter but an effect with a clear physical cause:

- **The "fat tail" of the kernel — the main cause.** The exponential kernel $e^{-\nu \cdot m}/r^2$ assigns non-zero dose to arbitrarily distant points, whereas the true β kernel **cuts off sharply at the extrapolated range**. For a single bead the dose is set by the near field (both models agree); as distant beads are added, the tail over-counts their contribution — the more so the larger the array. The monotonic growth 4 % → 19 % → 54 % is the direct signature of the effect. **The Loevinger kernel, falling off more steeply and cutting off near the range, is systematically closer to MC** (54 %→41 %, 19 %→9 %), which confirms the diagnosis.
- **The whole spectrum is described by one energy and one attenuation coefficient.** The classical model replaces the continuous β spectrum (many energies) by a single mean energy $\bar{E}$ and a single attenuation coefficient ν computed from the endpoint energy E_{max}. In reality soft β particles are absorbed near the surface while hard ones penetrate deeper, so the beam "hardens" with depth and the effective attenuation varies from point to point. A single averaged ν cannot capture this: it underestimates the fall-off with distance and therefore overestimates the far field (the contribution of distant beads).
- **Straight-line isotropic kernel, no scattering.** Multiple and back-scattering of electrons, which in the MC slightly reduce the far field, are not included; a second-order contribution.

Conclusion. The agreement at the level of the base source (hand calculation +9 %, sphere 4 %) confirms the physics and the normalization. The systematic overestimate of the classical method for packings is predictable and is explained by the known limitation of the dose kernel under superposition of extended sources; the more physical Loevinger kernel confirms this by approaching MC. In this regime the **Monte Carlo is the more reliable method** — the true finite beta range, the full spectrum and scattering are treated explicitly, not approximately. The result additionally rests on validated physics (G4EmStandardPhysics_option4, ENSDF/ICRP-107 spectra), statistical convergence (1σ < 1 %) and conservative assumptions (direct contact, sphere as a lower estimate), and the full openness of the project (`beads_skin`) allows every step to be re-checked. Nevertheless, the reported values remain a **model estimate**: methodological errors and input-data uncertainties cannot be excluded, so before practical use **independent verification by qualified specialists** and, where necessary, direct measurement with certified instruments are required (see the disclaimer at the top).

9 Comparison with regulatory limits

The relevant limit is the equivalent-dose limit **for skin** under Russian radiation safety standards NRB-99/2009[7]; it is defined as the dose $\dot{H}_p(0.07)$ averaged over 1 cm² at the basal-layer depth — exactly the quantity computed here. The general effective-dose limit (1 mSv/year for the public) does not apply directly to localized skin irradiation.

Table 8. Equivalent skin-dose limits (NRB-99/2009[7]) and contact time to the limit for the public (50 mSv/year).

Scenario	$\dot{H}_p(0.07)$, µSv/h	Hours to 50 mSv/year	Equivalent
single bead	6.7	≈ 7500	~20 h every day all year
chain (11)	18.3	≈ 2700	~7.5 h every day all year
dense mat	**48.4**	**≈ 1030**	**~2.8 h every day all year**

Equivalent skin-dose limits: **public 50 mSv/year**, **occupational (category A) 500 mSv/year**. Realistic handling regimes:

Table 9. Skin dose for typical regimes and fraction of the public limit (50 mSv/year).

Regime	Skin dose per year	Fraction of 50 mSv
jewelry (dense mat against skin) 2 h/day	≈ 35 mSv	71 % — below limit
jewelry (mat) 1 h/day	≈ 18 mSv	35 %
wearing a chain 24 h/day	≈ 160 mSv	320 % — above public, below occupational A
wearing a mat 24 h/day	≈ 424 mSv	848 % — above public, below occupational A (500)
single bead, episodic contact	≪ 1 mSv	negligible
pouring/sorting (minutes)	≪ 0.01 mSv	negligible

Conclusion. The contact dose rates (6.7–48 µSv/h) are not small in themselves, but the equivalent skin-dose limit is high (50 mSv/year for the public), so an appreciable dose accumulates only under **prolonged continuous direct contact** — many hours a day all year round. Normal handling (episodic contact, wearing the item a few hours a day) stays within the public limit. Even round-the-clock wearing of a dense packing directly on the skin (≈

424 mSv/year) exceeds the public limit but remains below the occupational category-A limit (500 mSv/year).

10 Assumptions and applicability

- **Broken equilibrium.** It is assumed that radium and the subsequent chain members are absent (purified uranium). Residual ^{226}Ra (partial equilibrium) would add penetrating series gamma radiation — a separate source, not included here. For radium-bearing glass the picture would change qualitatively.
- **Glass density** 2.5 g/cm³ — an assumption; it weakly affects beta self-absorption, since at fixed measured mass and outer diameter the areal density of the glass barely depends on density.
- **Bead shape.** The 6/0 rocaille is modelled as a Ø4.1 mm sphere with an axial hole at the measured mass; the real shape (a rounded barrel) is intermediate between a sphere and a cylinder, so the true dose lies between the spherical estimate (this work) and the cylindrical one (~20 % higher for a single bead; the difference is small for a dense packing).
- **Cerium content** ~0.5 % (exact value unknown); no effect on β/γ transport at this level.
- **Direct contact** is the conservative (maximum) case of skin dose. Any gap (clothing fabric, a mount, a dust layer, lacquer) sharply reduces the electron component (> 99.8 % of the dose): the beta range in dense material is fractions of a millimetre.
- **The limit for hands/feet** is also 50 mSv/year (public) — the same order, relevant for prolonged holding of the beads in the hands.

11 Statement on the use of AI

The work was carried out by an "operator + AI agent" pairing (Claude Code interface, Anthropic). Roles:

- **Calculation line** (source model, geometry and physics in Geant4, C++ code, runs, Python post-processing and convolution, illustrations and 3D field visualization, article text) — the Claude Code AI agent; Anthropic Claude Opus 4.8 and Claude Fable 5 models.
- **Independent audit** — a separate AI agent (Anthropic Claude): a fact- and methodology-based review. It independently reproduced the doses from the raw calculation data and identified a normalization error in the first revision (double counting of the isobaric sub-chain when summing overlapping runs): the chain-limiting command has no effect in Geant4 analog mode, so the ^{234}Th run already contained the ^{234m}Pa contribution. The fix — summing only over the two non-overlapping chains (A = 234, A = 235). The qualitative conclusions were unchanged (the error was on the conservative side).
- **Operator (human):** provided the sample and its characteristics, measured by colleagues via gamma-ray spectrometry on an HPGe detector[14] (specific activities ^{238}U/^{235}U, mass, geometry), set the task, chose and confirmed the assumptions, accepted each step, made critical remarks, and made the publication decisions. Responsibility for the input assumptions and final conclusions rests with the operator.

All reported values are reproducible with the attached code (project `beads_skin`). An interactive $\dot{H}_p(0.07)$ calculator accompanies this paper, covering arbitrary packing geometry, uranium content and bead size (described in § 4); its kernel is calibrated against the reference points of the present work and runs entirely in the reader's browser.

12 References, data and code

1. Strahan D. Uranium in glass, glazes and enamels: history, identification and handling. *Studies in Conservation*, 46(3), 2001, 181–195. Used: typical uranium content of glass up to ~1.4–2 wt% (our sample 1.85 %). tandfonline (https://www.tandfonline.com/doi/abs/10.1179/sic.2001.46.3.181)

2. Bamford C.R. *Colour Generation and Control in Glass*. Elsevier, 1977. Used: CeO_2 as a glass decolorizer.

3. Cerium decolorizing mechanism ($Fe^{2+} \rightarrow Fe^{3+}$ oxidation) and typical CeO_2 fractions 0.025–0.2 wt%: review "Use of cerium oxide as decolorant in the glass industry"; Stanford Advanced Materials. ResearchGate (https://www.researchgate.net/publication/294227162_Use_of_cerium_oxide_as_decolorant_in_the_glass_industry)

4. **IAEA Nuclear Data Services, Live Chart of Nuclides** (ENSDF-based). Decay data (half-lives, β endpoints, γ lines) for ^{234}Th, ^{234m}Pa, ^{235}U, ^{231}Th, ^{230}Th obtained directly via the API (relnsd/v1). Used: ^{234m}Pa $Q_\beta \approx 2.27$ MeV; ^{235}U γ 143.8/163.4/185.7/205.3 keV (185.7 = 57.2 %); ^{234}Th γ 63.3 keV; ^{231}Th Q_β 391.5 keV; ^{230}Th T½ 75,584 y. nds.iaea.org — Live Chart (https://www-nds.iaea.org/relnsd/vcharthtml/VChartHTML.html)

5. ICRP Publication 107. *Nuclear Decay Data for Dosimetric Calculations*. Ann. ICRP 38(3), 2008. icrp.org (https://www.icrp.org/publication.asp?id=ICRP%20Publication%20107)

6. Evaluated Nuclear Structure Data File (ENSDF), NNDC, Brookhaven National Laboratory. nndc.bnl.gov/ensdf (https://www.nndc.bnl.gov/ensdf/)

7. ICRP Publication 103. *The 2007 Recommendations of the ICRP*. Ann. ICRP 37(2–4), 2007. Used: skin dose averaged over 1 cm² at 70 μm (7 mg/cm²). icrp.org (https://www.icrp.org/publication.asp?id=ICRP%20Publication%20103)

8. Radiation Safety Standards NRB-99/2009 (SanPiN 2.6.1.2523-09), Russia. Skin limits: public 50 mSv/year, occupational A 500 mSv/year. PDF (https://www.ntcexpert.ru/documents/docs/nrb-99-2009.pdf)

9. ICRU Report 44. *Tissue Substitutes in Radiation Dosimetry and Measurement*. 1989. icru.org (https://www.icru.org/report/tissue-substitutes-in-radiation-dosimetry-and-measurement-report-44/)

10. Agostinelli S. et al. Geant4 — a simulation toolkit. *Nucl. Instrum. Meth. A* 506(3), 2003, 250–303. doi:10.1016/S0168-9002(03)01368-8 (https://doi.org/10.1016/S0168-9002(03)01368-8)

11. Allison J. et al. Recent developments in Geant4. *Nucl. Instrum. Meth. A* 835, 2016, 186–225. doi:10.1016/j.nima.2016.06.125 (https://doi.org/10.1016/j.nima.2016.06.125)

12. Geant4 Physics Reference Manual (v11.2). geant4.web.cern.ch (https://geant4.web.cern.ch/)

13. Bourdon B. et al. (eds). *Uranium-series Geochemistry*. Rev. Mineral. Geochem. 52, 2003. doi:10.1515/9781501509308 (https://doi.org/10.1515/9781501509308)

14. Hamby D.M. et al. VARSKIN — skin contamination dosimetry. NUREG/CR-6918. Methodological analogue; no comparison performed here. nrc.gov (https://www.nrc.gov/reading-rm/doc-collections/nuregs/contract/cr6918/)

15. Sample data — specific activities $^{238}U/^{235}U$, mass and geometry ("Petri dish") measured by colleagues via high-resolution gamma-ray spectrometry on an HPGe (high-purity germanium) detector; provided to the operator (internal, 2021).

16. $^{90}Sr/^{90}Y$ surface-contamination skin-dose factor (order-of-magnitude check, §8): Colorado State Univ., Radiation Safety Module 5; Stanford EH&S ^{90}Sr Safety Data Sheet. colostate (http://www.ehs.colostate.edu/_PDF/Rad/Mod-5.pdf) · stanford (https://ehs.stanford.edu/wp-content/uploads/Sr-90-RSDS.pdf)

17. Hassan H.J., Hashim S. et al. Naturally Occurring Radioactive Materials in Bracelets and Necklaces: Radiological Risk Evaluation. *Int. J. Environ. Res. Public Health* 18(21), 2021, 11170. Analogous study (HPGe + Geant4 MC of NORM jewelry): their items are radium-bearing (U/Th series intact, Th-dominant) and the gamma dose was assessed → skin equivalent dose 0.04–0.42 μSv/h (source Table 3, max sample N16); our purified-U beta-dominated beads → higher skin dose but no penetrating series γ. doi:10.3390/ijerph182111170 (https://doi.org/10.3390/ijerph182111170)

18. Loevinger R. The dosimetry of beta sources in tissue. The point-source function. *Radiology* 66(1), 1956, 55–62. Used (§7.2): the beta point-source dose function Φ(x), including the Loevinger form, and the empirical β attenuation coefficient. doi:10.1148/66.1.55 (https://doi.org/10.1148/66.1.55)

19. Cember H., Johnson T.E. *Introduction to Health Physics*, 4th ed. McGraw-Hill, 2009, "Beta dosimetry" chapter. Used (§7.1): working β-dosimetry formulas — the apparent attenuation coefficient $\nu = 16(E_{max} - 0.036)^{-1.4}$ cm²/g; the equilibrium absorbed dose in an infinite medium $\dot{D}_\infty = C_\nu \cdot \bar{E}$ and its half at the surface of a semi-infinite source.

20. Cross W.G., Freedman N.O., Wong P.Y. Beta-ray dose distributions from point sources in an infinite water medium. *Health Physics* 63(2), 1992, 160–171. Used (§7.2): the beta **point-dose-kernel** method — the $1/(4\pi r^2)$ geometric spreading with a radial fall-off function; reference dose distributions around a point source in water. PubMed 1399614 (https://pubmed.ncbi.nlm.nih.gov/1399614/)

Calculation code and data: Geant4 project `beads_skin` (main.cc, convolution `postproc_beads.py`, renderers `field_render.py`, `fig_hotparticle.py`). All graphics are in the `figures/` folder of this page.

Appendix A. Conversion from β flux density to the skin dose-equivalent rate $\dot{H}_p(0.07)$ (dense packing)

For field monitoring it is convenient to relate the reading of the **β-particle flux density** φ_β (measured with β flux-density instruments, e.g. a **BDPB** detector unit or an **MKS-01SA** dose-rate/radiometer) to the skin dose-equivalent rate. For the dense-packing geometry:

$$\dot{H}_p(0.07) = K \cdot \varphi_\beta$$

Flux density — direct Monte Carlo. In the same Geant4 model (§3), for the 9×9 mat the β particles crossing the skin boundary (over the 1 cm² disk) were counted and folded with the measured activities (as for the dose). The **156 keV** registration threshold is applied (soft β are cut by the instrument):

Table A1. β flux density from the dense-packing surface (direct Geant4 transport).

Quantity	β·cm^{-2}·s^{-1}	β·cm^{-2}·min^{-1}
all β	17.9	1070
β > 156 keV (BDPB threshold)	**16.4**	**983**

Cross-check against measurement. The operator measured the sample (beads in a Petri dish) with a β flux-density instrument: **≈ 1200 β·cm^{-2}·min^{-1}**. The direct calculation gives ≈ 1000–1070 β·cm^{-2}·min^{-1} — agreement within ~15 % (the dish sample is somewhat denser than the modelled single-row mat), which **independently confirms the transport model**.

The coefficient. With $\dot{H}_p(0.07)$ of the dense packing = 48.4 μSv/h (Monte Carlo, §4) and φ_β(>156 keV) = 16.4 β·cm^{-2}·s^{-1}:

$$\mathbf{K \approx 3.0\ (\mu Sv/h)/(\beta \cdot cm^{-2} \cdot s^{-1})} \quad \text{or} \quad \mathbf{K \approx 0.05\ (\mu Sv/h)/(\beta \cdot cm^{-2} \cdot min^{-1})}$$

Rule of thumb: **1000 β·cm^{-2}·min^{-1} ≈ 50 μSv/h**. Uncertainty ~30 % (glass density ±10 %, MC statistics, measurement geometry and backscatter). *Note.* A simple analytical "net current" estimate $J = C_m \cdot n_\beta/(6v)$ = 7.5 β·cm^{-2}·s^{-1} gives half as much: a detector counts *all crossings* (≈ 2× the net current for a broad angular distribution) plus conversion electrons — hence direct transport, consistent with the measurement, is used.

How to use. Measure the β flux density with a BDPB (or MKS-01SA) on the surface of a dense-packing item (embroidery, tight beading) and multiply by K. Notes: **(1)** the coefficient is derived for a *dense packing* (quasi-infinite plane); for a single bead or a sparse layout the local "flux ↔ dose" relation differs. **(2)** The instrument registers the 2π surface emission — use the instrument's own flux-density calibration. **(3)** Both instruments measure the β flux density in the same units — **min^{-1}·cm^{-2}**: the BDPB-01 (ATOMTEX) registers β at 0.156–3.54 MeV and is calibrated with ^{90}Sr+^{90}Y; the MKS-01SA (SNIIP AUNIS) covers 5–3·10^4 min^{-1}·cm^{-2}. E_{max} of ^{234m}Pa (2.27 MeV) lies within the working range of both, and the spectrum is close to ^{90}Y (2.28 MeV) → the energy response nearly coincides, so the standard calibration applies directly. **(4)** The geometry is direct contact (a conservative estimate). Calculation: script `handcalc_flux.py` of the `beads_skin` project.

The calculation was performed by an AI agent (Anthropic Claude) under the guidance and control of the operator. Method — direct Monte Carlo radiation transport (Geant4 11.2.1) with convolution by measured activities. Values are for the conservative direct-contact geometry.

VibeEngineering · 23 Jul 2026 · uranium-bead dosimetry · rev. 5 (problem→solution→verification→analysis structure; quantity $\dot{H}_p(0.07)$; hand classical calculation; UDC index)